

Fig. 1 — Block diagram of device for setting currents at various stages of a short circuit. 1 — Transformer; 2 — thyristor rectifier; 3 — adjustable resistor; 4 — welding arc; 5 — shunt; 6 — feedback circuit; 7 — single plate microprocessor.

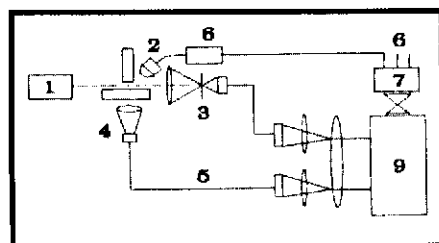


Fig. 2 — Schematic illustration of apparatus for laser back-light high-speed photography that records two images simultaneously with arc sound and voltage oscillographs. 1 — laser back light; 2 — microphone; 3 — aperture; 4 — lens; 5 — optical fiber; 6 — magnifier with band filter; 7 — light oscillograph; 8 — arc voltage signal; 9 — high-speed camera.

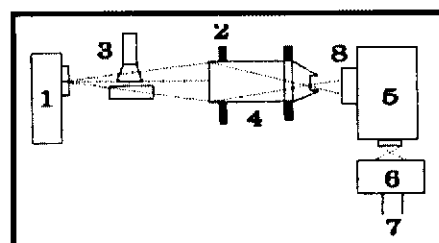


Fig. 3 — Schematic illustration of apparatus for x-ray back-light high-speed photography. 1 — X-ray tube; 2 — lead shelter; 3 — electrode; 4 — image magnifier; 5 — high-speed camera; 6 — light oscillograph; 7 — arc voltage and sound signals; 8 — lens.

$$E_o = C_c/100 - \sum (C_m \times M_c \times Y)/(W_a \times X)$$

where:  $E_o$  represents quantity in moles of the remaining  $CO_2$ , calculated by subtracting quantity of  $CO_2$  that could be de-

oxidized by alloying elements from that of the total  $CO_2$  evolved from marble in 100-g covering;  $C_c$  is marble wt-%; 100 is molecular weight of marble ( $CaCO_3$ );  $C_m$  is the wt-% of a deoxidizer;  $M_c$  is the wt-% of alloying element in the deoxidizer;  $W_a$  is the atomic weight of the alloying element;  $X, Y$  are the ratio of the numbers of atoms in the oxide  $M_xO_y$ .

The second series of electrodes contained up to 3.5% of three types of rare earth metal additives, i.e., lanthanum oxide, a mixed oxide of rare earth metals, and an alloy of heavy rare earth metal. The compositions of the covering are shown in Table 3. The compositions of the test pieces are shown in Table 4.

#### Device

Figure 1 shows the block diagram of a device made for setting currents at various stages of a short circuiting process. At the beginning and the ending of a short circuit, the arc voltage drops down and then rises up abruptly. A single plate microprocessor accepts these signals and controls a trigger circuit of a thyristor rectifier welding machine. The currents at 1) the beginning of a short circuit, 2) during the overall period of short circuiting, including its breaking stage and 3) at the re-initiating stage, could be set.

A device was made to record and statistically analyze the parameters of the short circuiting process. Histogram of event numbers against the duration of the short circuits could thus be obtained. Short circuits with a duration of less than 2 ms were referred to as instantaneous short circuits.

An apparatus for laser backlight, high-speed photography was used (Ref. 4). Using this apparatus, high-speed pictures (1000–2000f/s) with simultaneous recording of a metal transfer image, arc side image, arc sound oscillograph, and arc voltage oscillograph could be obtained. Figure 2 shows a schematic illustration of the apparatus.

An apparatus for x-ray, back-light, high-speed photography was used to observe gas bubbles forming and evolving in drops of melted metal or weld pools. Figure 3 shows its schematic illustration. De-

tailed information on the high-speed photography can be obtained from Ref. 4.

#### Spatter Collection

All welding was carried out on plates (100 x 300 x 10 mm) put in an open box (400 x 500 x 200 mm) using 170 A direct current electrode positive (DCEP) welding current and an arc voltage of 23–24 V in a flat position. All of the spatter deposited on the plate and in the box was collected. The slag on the surface was detached by grinding and metal drops were collected by a magnet. The coefficient of spatter was defined as the ratio of the weight of spatter to that of the consumed core wire of electrodes.

#### Results of Experiments

##### 1) Effect of the current at the beginning stage of a short circuit upon the quantity of spatter

The welding condition was set with a welding current of 170 A, arc voltage of 23–24 V and short circuiting current of 250 A, using commercial basic electrodes. Peak current at the beginning stage (within 4.5 ms) was set at 50, 100, 150, 200, 250, 300, 350, and 400 A, respectively. The oscillographs of the current and the voltage are schematically shown on Fig. 4. The spatter coefficients are plotted against the peak currents at the beginning stage of the short circuiting process in Fig. 5. In the same diagram the curves drawn indicate the event numbers of the short circuits with a duration of 2–5 ms and that less than 2 ms (instantaneous).

##### 2) Effect of current at the arc re-initiating stage after short circuiting on the quantity of spatter

At the arc reinitiating stage, the gas in the atmosphere around it is heated and expands abruptly. It is believed that the expanding gas has a strong impact on the weld pool, which results in spatter. To determine if this idea was valid, the currents at the arc reinitiating stage were set to 50, 100, 200, 300, and 400 A. The arc currents and voltage oscillographs were schematically shown in Fig. 6. The spatter coefficients are plotted against the cur-

Table 1 — Compositions of Core Wires (wt-%)

Type	C	Mn	Si	S	P
H08A	0.06	0.45	0.01	0.03	0.03
H08MnA	0.07	1.05	0.06	0.03	0.03
H08Mn <sub>2</sub> Si	0.07	2.05	0.76	0.03	0.03

Diameter 4.0 mm.

Table 2 — Compositions of Electrode Coverings with Various Oxygen Potential (wt-%)

Fluor-spar	Titanium dioxide	Sodium carbonate	Fe-Ti	Powder of Fe	Marble	Fe-Mn	Fe-Si	$E_o$
35	3	2	3	13	40	0	0	0.37
35	3	2	3	13	35	3.5	1.5	0.22
35	3	2	3	13	30	7.0	3.0	0.07
35	3	2	3	13	25	10.5	4.5	-0.08
35	3	2	3	13	20	14.0	6.0	-0.23
35	3	2	3	13	15	17.5	7.5	-0.37

Fe-Ti with 38%Ti, Fe-Mn with 78%Mn, Fe-Si with 48%Si. Bonding agent is 27% water glass, diameter 6.4 mm.







Fig. 13 — Typical processes of short circuit breakage taken by laser back-light, high-speed photography (200/s). On right side is the main image of the liquid metal bridge and the process of breaking (time sequence is from upper to lower). On left side, the moment the short circuit breaks, the arc voltage jumps from the short circuiting voltage to the arc voltage, as shown by the thick line. The arc sound oscillograph vibrates violently, shown by the thinner line, as the explosion occurs at that moment. The light spots appear after that moment showing the reinitiation of the arc.

the most important one for decreasing spatter production.

The main process resulting in the spatter is the CO gas explosion. High current at this moment enhances this process and enlarges its effect.

In Fig. 12, the diameters of the metal bridges measured just prior to short circuit breakages increase with increasing rare earth metal agent contents. Spatter quantity variation coincides with that of diameters of the metal bridge. According to the electric explosion viewpoint, the spatter is caused by a high density of short circuiting current which overheats the metal bridge. It can, therefore, be concluded that the thinner the metal bridge, the higher the current density and the heavier the spatter. However, the experimental results in present work run counter to this conclusion. So the electrical explosion is not the main process of the spatter produced in SMAW with

basic electrodes.

Figure 11 shows the experimental results of the combining effect of oxygen potential and the short circuiting current upon spatter. The electrode with a ratio of marble to deoxidant of 40:0 in the covering represents electrodes with high oxygen potential. Curve 1 presents the spatter produced when it is welded with various short circuiting currents. The electrode with ratio of marble to deoxidant content of 15:25 has a very low oxygen potential, and the spatter produced by it (shown by Curve 2) can reasonably be assumed to be caused by an electric effect. If 2% is taken to be an intrinsic spatter coefficient caused by random factors, Curve 4 in Fig. 11 (by subtracting 2% from Curve 2) represents the spatter caused by increasing the short circuiting current only. Curve 3 is obtained by subtracting 2% of intrinsic spatter and subtracting Curve 4, the spatter

caused by electrical effect, from Curve 1. It is taken as the spatter caused by the explosion of CO gas at various short circuiting current levels. It is apparent that the spatter quantity caused by gas explosion (Curve 3) is much higher than that caused by increasing the short circuiting current alone (Curve 4). Curve 3 also shows a significant increase in spatter with an increasing of short circuiting current, which means that the high short circuiting current enhances the gas explosion and enlarges its effect on spatter. Since under normal SMAW conditions the short circuiting current is about 250 A, the spatter caused by sole electrical effect is low (Curve 4). The high spatter shown by Curve 1 is caused mainly by the gas explosion.

Figure 12 shows that the rare earth metal oxides increase spatter, however, the rare earth metal alloys decrease the spatter. This phenomenon is consistent

